

Advanced characterization of particles triboelectrically charged by a two-stage system with vibrations and external electric fields

Megumi Mizutani, Masatoshi Yasuda, Shuji Matsusaka *

Department of Chemical Engineering, Kyoto University, Kyoto 615-8510, Japan

Abstract

In this study, we propose a new method to effectively characterize particle tribocharging caused by repeated contact with a wall in an external electric field. We perform experiments using a two-stage system consisting of two inclined vibrating plates and electrodes. The mass flow rate and charge of particles were controlled at the first vibrating plate, and the charge that was transferred from the plate to the particles was obtained from the difference between the charges on particles at the lower and upper ends of the second vibrating plate. In addition, electric currents generated by the charge transfer were simultaneously measured at the second vibrating plate. From these measurements, we verified that the charge balance in this system holds. Furthermore, we found that the charge transfer depends on various factors, such as the initial charge, chemical and electrical properties, travel length of particles, and the external electric field. We also found that the equilibrium charge of particles depends on the chemical property and external electric field. The equilibrium charge and the rate of tribocharging were evaluated analytically from the relationship between the initial and transferred charges without changing the travel distance of particles. This method enables the rapid and reliable analysis of the particle tribocharging process.

Keywords: Particle tribocharging; Repeated contact; Vibration; Electric field; Initial charge

* Corresponding author. *E-mail address:* matsu@cheme.kyoto-u.ac.jp (S. Matsusaka)

1. Introduction

When two different materials are brought into contact with each other, an electric charge is transferred from one to the other. This phenomenon is called “contact electrification” or “contact charging.” When they are rubbed against each other, it is called “triboelectric charging,” or simply “tribocharging.” With respect to brief contact made during collisions, it can be called “impact charging” [1, 2]. In practice, it is not easy to classify the contact states into groups, such as sliding, rolling, and impact; thus, the term “tribocharging” is used in such general cases. If the materials are insulators, charges remain on the surfaces. As a result, the electrostatic phenomena that occur with solid particles are significant as the specific surface area increases. For example, electrostatic forces acting on charged particles affect powder flowability [3–7] and segregation [8]. In addition, excessively charged particles cause an electrostatic discharge, which can pose the risk of fire and explosion hazards [9]. On the other hand, charged particles can be used for many industrial applications, including electrophotography [10], electrostatic powder coating [11], electrostatic separation [12, 13], self-assembly [14], and various measurements [15–17].

In industry, the characterization and control of particle tribocharging are essential to maintain powder processes in normal operating conditions, and to maximize the performance of various pieces of equipment. The cascade method to measure the charge of particles cascading down an inclined plate has often been used for characterizing particle tribocharging because of its ease of operation [18–20]. However, the motion of small particles that are on the surface is disturbed by adhesive forces such as van der Waals forces [21] and electrostatic forces [22–25]. To overcome these adhesive forces, external forces should be applied continuously [26, 27]. For example, particles have been charged by repeated contact on a vibrating feeder [28] or in a shaker [29, 30]. Otherwise, particles have been charged in gas-solid pipe flows without using vibration [31], and the frequency of particle–wall contacts may be increased by applying a centrifugal force to the particles in a rotational flow [32–34]. Furthermore, because particle tribocharging is affected not only by the material property but also by the electric field [35], the charges on the particles can

be altered by changing the electric field.

In one study, the authors expanded the range of the particle charge and improved the controllability by applying an external electric field to the particle tribocharging caused by repeated contact under vibration [36], and they also proposed a two-stage system with a pre-charging stage for controlling the initial charge and mass flow rate of particles [37]. In this system, the particle tribocharging was analyzed by measuring the charge on particles using a Faraday cup. If electric currents are measured online, the procedure will be simplified and the analysis will be more flexible.

In this study, we modify the two-stage system used to characterize particle tribocharging in order to measure electric currents as well as particle charges, and then evaluate the performance of the modified system. Next, we analyze in more detail the equilibrium charge of particles and the rate of tribocharging to better understand the particle tribocharging caused by repeated contact. Finally, we propose a new method to characterize the particle tribocharging on the basis of the theoretical analysis taking into account the initial charge of particles and the external electric field.

2. Theoretical model

2.1. Basic concept of particle tribocharging caused by repeated contact

The theoretical model of the particle tribocharging has been reported elsewhere [1, 2, 33]. Here, we describe the basic concept used to analyze the particle tribocharging caused by repeated contact with a wall in an external electric field. The total potential difference V at the contact gap, which is the driving force for charge transfer, is expressed as

$$V = V_c - V_e - V_b + V_{\text{ex}}, \quad (1)$$

where

$$V_e = k_e q, \quad (2)$$

$$V_b = k_b q, \quad (3)$$

and

$$V_{\text{ex}} = k_{\text{ex}} z_0 E_{\text{ex}}, \quad (4)$$

where V_c is the potential difference based on the surface work functions, and V_e and V_b are the potential differences arising from the image charge and the space charge caused by the surrounding charged particles, respectively, which act as an inhibitor for the particle tribocharging caused by repeated contact. k_e and k_b are constants, q is the charge on the particle, and V_{ex} is the potential difference arising from the external electric field. V_{ex} does not depend on q , and has the same effect as V_c . When the sum of V_c and V_{ex} has a positive value, the particle tends to acquire a positive charge. k_{ex} is a constant, z_0 is the effective contact gap including the surface roughness, and E_{ex} is the external electric field. When the wall is a positive electrode, E_{ex} in Eq. (4) becomes larger than zero, and the particle is able to acquire a positive charge more easily.

When the charge transferred between the contact surfaces is proportional to both the total potential difference V and the capacitance C , the continuous quantity dq/dn is expressed as

$$\frac{dq}{dn} = k_c CV, \quad (5)$$

where n is the number of particle-wall contacts and k_c is a constant, i.e., charging efficiency. Assuming that the number of particles is sufficiently small, and thus the space charge is negligible, by solving Eq. (5) with the initial condition $q = q_0$ at $n = 0$, we obtain the following exponential equation:

$$q = q_0 \exp\left(-\frac{n}{n_0}\right) + q_\infty \left\{1 - \exp\left(-\frac{n}{n_0}\right)\right\}, \quad (6)$$

where

$$q_\infty = \frac{V_c + V_{\text{ex}}}{k_e} = \frac{V_c + k_{\text{ex}} z_0 E_{\text{ex}}}{k_e} \quad (7)$$

and

$$n_0 = \frac{1}{k_e k_c C}, \quad (8)$$

where q_∞ is the equilibrium charge of the particle and n_0 is the characteristic number of the particle tribocharging.

2.2. Method for characterizing particle tribocharging caused by repeated contact

When particles are traveling on an inclined vibrating plate, it can be assumed that the frequency of the particle-wall contacts per unit length is constant, and that the number of contacts n is proportional to the length, L . Then, on the basis of Eq. (6), the charge-to-mass ratio of the particles, q_m , i.e., the specific charge, is expressed as

$$q_m = q_{m0} \exp\left(-\frac{L}{L_0}\right) + q_{m\infty} \left\{1 - \exp\left(-\frac{L}{L_0}\right)\right\}, \quad (9)$$

where L_0 is the characteristic length of particle tribocharging, q_{m0} is the initial specific charge, and $q_{m\infty}$ is the equilibrium specific charge, which is obtained from Eq. (7), i.e.,

$$q_{m\infty} = \frac{V_c + V_{\text{ex}}}{k_e m_p} = \frac{V_c + k_{\text{ex}} z_0 E_{\text{ex}}}{k_e m_p}, \quad (10)$$

where m_p is the mass of the particle. Here, it should be noted that the equilibrium specific charge, $q_{m\infty}$, has a linear relationship with the external electric field, E_{ex} .

The variation of the specific charge caused by repeated contact between the particles and the plate, i.e., the transferred specific charge, Δq_m , is obtained from Eq. (9), i.e.,

$$\begin{aligned} \Delta q_m &= q_m - q_{m0} \\ &= q_{m\infty} \left\{1 - \exp\left(-\frac{L}{L_0}\right)\right\} - q_{m0} \left\{1 - \exp\left(-\frac{L}{L_0}\right)\right\} \\ &= (q_{m\infty} - q_{m0}) \left\{1 - \exp\left(-\frac{L}{L_0}\right)\right\} \end{aligned}$$

$$= a q_{m0} + b, \quad (11)$$

where

$$a = \exp\left(-\frac{L}{L_0}\right) - 1 \quad (12)$$

and

$$b = -a q_{m\infty}. \quad (13)$$

The transferred specific charge, Δq_m , has a linear relationship with the initial charge, q_{m0} . The coefficient of the linear term, a , is expressed as an exponential function of the length, L . Therefore, the characteristic length, L_0 , is represented by

$$L_0 = -\frac{L}{\ln(1+a)} \quad (14)$$

Furthermore, for $L > 0$, the following equation holds irrespective of L .

$$\text{For } \Delta q_m = 0, \quad q_{m\infty} = q_{m0} \quad (15)$$

Using Eq. (15), the equilibrium specific charge, $q_{m\infty}$, is determined from the experimental data.

3. Experiment

3.1. Materials

We used spherical particles in order to conduct experiments under stable conditions. The materials were glass, manganese ferrite, and manganese ferrite coated with fluorine polymer. **Fig. 1** shows the SEM images of these particles. The surface of the glass beads was smooth, but the manganese ferrite particles and those coated with polymer have rough surfaces. In these SEM images, the manganese ferrite appeared to be light gray, while the polymer was dark gray. From the difference in the lightness, we deduced that the polymer sufficiently covers the manganese ferrite particles.

To obtain the particle size distributions, 1000 projected area diameters were measured for each

sample by performing digital processing of the SEM images. The count median diameter of the glass beads, D_{p50} , was 101 μm , and the standard deviation, σ_g , was 1.1. For the manganese ferrite particles, $D_{p50} = 81 \mu\text{m}$ and $\sigma_g = 1.2$, while for the manganese ferrite particles coated with polymer, $D_{p50} = 82 \mu\text{m}$ and $\sigma_g = 1.2$. These manganese ferrite particles had voids inside, and thus the particle density was smaller than the true density. The size distributions and their physical properties are summarized in **Table 1**.

To obtain the electrical property of the particles, we measured the volume resistivity of the particles packed in a cylindrical cell that was 35 mm high and 40 mm in diameter. Because the volume resistivity depends on the packing condition, we compressed the particles at a constant pressure of 5 MPa. The value of each resistivity was calculated from the voltage measured in the range from 1 nA to 100 μA . As shown in Table 1, the glass beads have larger resistivity and the manganese ferrite particles have smaller resistivity. The manganese ferrite particles coated with polymer have an intermediate value.

3.2. Experimental setup and procedure

Fig. 2 shows the schematic diagram of the experimental setup that was used to characterize particle tribocharging caused by repeated contact in an external electric field. The test section consists of two inclined vibrating plates with electrodes. The first plate plays the role of the controller of the mass flow rate and the particle charge, while the second plate is used to characterize the particle tribocharging.

The first plate was 15 mm wide and 80 mm long, and was made of austenitic stainless steel. At its upper end, a short pipe for containing particles was placed with a gap less than 0.5 mm. The particles were fed to the first plate through a 1.2-mm-diameter hole in the bottom of the short pipe. The feed rate was controlled by the gap distance and the amplitude of the vibrations applied to the short pipe and plate [38, 39]. These vibrations were applied at 300 Hz in the longitudinal

direction of the plate. In this study, the particle feed rate was set at less than 10 mg/s in order to prevent collisions between the particles on the vibrating plate. An electric field controlling the particle tribocharging was formed by applying a voltage to an upper electrode with a length of 50 mm, which was placed at a distance of 5 mm above the first vibrating plate. The vibrating plate was grounded to enable its use as the lower electrode. The specific charge of the particles at the end of the first vibrating plate was measured by a Faraday cup connected to an electrometer. **Fig. 3** shows the values of the specific charge measured at different electric field strengths. The specific charge is seen to vary linearly with the electric field. Therefore, the charges on the particles can be arbitrarily set by changing the electric field.

The second inclined plate was made of austenitic stainless steel, which was the same as that for the first plate. However, a different flat material could be attached on the second plate. Experiments performed using a metal plate coated with a 25- μm -thick polyimide film were also carried out. Although polyimide is a dielectric material, the charge accumulated on the surface can pass through the film because of the breakdown when the film thickness is as small as 25 μm [35]. Therefore, the experiments performed using polymer film could be conducted without any problems. Vibrations for the second plate were applied in the tangential direction to the plate in order to induce particle saltation and tribocharging caused by repeated contact with the plate. The frequency of vibration is the same as that for the first vibrating plate.

Fig. 4 shows the displacement of the second vibrating plate as a function of time. The plate moved sinusoidally in synchronization with the applied AC signals. To control the movement of the two vibrating plates, a control unit (VST-01, IMP Co., Ltd.) was used. The two vibrating plates were placed at an inclination angle of 30° to transfer the particles downward under gravity.

To investigate the effect of the travel distance of particles in the electric field on particle tribocharging, electrodes with different lengths (20, 40, 65, 80, and 100 mm) were placed over the second inclined vibrating plate at a distance of 5 mm from the plate. The vibrating plate was grounded for use as the lower electrode, and an electric field was formed between the upper and

lower electrodes. With the exception of the upper electrodes, all of the metal parts were grounded to avoid charge accumulation. When the polarity of the particle charge differs from that of the upper electrode, the particles have upward electrostatic forces caused by Coulomb forces. When the external electric field is too strong, the particles contact the upper electrode. To avoid this problem, we used the electric field in the range from -200 kV to 200 kV.

The particles falling from the lower end of the first inclined vibrating plate were fed to the position close to the upper end of the upper electrode of the second vibrating plate. The charge of the particles after passing through the second vibrating plate was measured by the Faraday cup. The charge transferred from the plate to the particles, Δq_m , was calculated from the difference between the particle charges at the lower and upper ends of the second vibrating plate. In addition, another electrometer was connected to the second vibrating plate to measure the electric currents, and the charge on the particles after passing through the vibrating plate was calculated by performing time integration of the electric currents, which were recorded into the computer every 50 ms. The transferred specific charge, Δq_m , was calculated using the following equation:

$$\Delta q_m = -\frac{\int_{t_0}^{t_1} Idt}{\int_{t_0}^{t_1} w_p dt} = -\frac{\int_{t_0}^{t_1} Idt}{M_t} \quad (16)$$

where t is the time, I is the electric current, w_p is the mass flow rate of particles, and M_t is the total mass of the particles.

The behavior of the particles on the second plate was observed at the lower end from the tangential and normal directions to the vibrating plate through a high-speed microscope camera with a resolution of $1 \mu\text{m}$ (Fastcam-Max, Photron). All of the experiments were carried out under room conditions, i.e., temperature: $17\text{--}22$ °C and relative humidity: $20\text{--}40\%$.

4. Results and discussion

4.1. Simultaneous measurement of electric charge and current

Fig. 5 shows the electric currents detected at the second inclined vibrating plate. The manganese ferrite particles and the stainless steel were used for this experiment. The distance traveled by the length of particles was 65 mm, the initial specific charge was $-2 \mu\text{C}/\text{kg}$, and the mass flow rate was 6 mg/s. After feeding, electric currents were detected as a result of the charge transfer caused by repeated contact between the particles and the plate. When the particles obtain positive charges from the plate, the particles lose negative charges and negative currents are detected. Although small fluctuations were seen in this figure, the values for each measurement were almost constant.

Fig. 6 shows a comparison of the transferred specific charges, Δq_m , obtained by the time integration of the electric current and the difference in the charges measured by the Faraday cup. These experimental results were obtained using various materials. From this figure, it was found that the values obtained by different methods are in reasonable agreement with each other and that the charge balance in this system holds. When the particles move successively on the first and second inclined vibrating plates, we can easily measure the charge of the particles falling from the lower end of the second inclined vibrating plate, but it is difficult to simultaneously measure the initial charge of the particles fed to the second vibrating plate. On the other hand, the electric currents can be measured simultaneously at the second vibrating plate. Therefore, the initial charge of the particles can be calculated using the charge balance based on a combination of the time integration of electric current and the charge measurement at the lower end.

4.2. Particle charge profile

Fig. 7 shows experimental results for particle charge profiles, i.e., relationships between the specific charge of particles and the length of the electrode as a function of the external electric field and initial specific charge. The materials of the particles and the second plate were

manganese ferrite and stainless steel, respectively. This figure indicates that the specific charge approaches an equilibrium charge depending on the external electric field, irrespective of the initial specific charge.

We analyze these particle charge profiles using the theoretical model mentioned in Section 2.2. The specific charge, q_m , can be expressed by Eq. (9). The solid lines in Fig. 7 were obtained by fitting this equation. The fitting parameters were the equilibrium specific charge, $q_{m\infty}$ and the characteristic length, L_0 . These parameters are essential for quantitative characterization of the particle tribocharging. To determine the fitting parameter, L_0 , with high accuracy, the initial charge should be set largely apart from the equilibrium charge. The proposed two-stage system enables us to easily change the initial charge, and will be effective for characterizing the particle tribocharging.

4.3. Transferred specific charge and initial specific charge

Fig. 8 shows the relationship between the transferred specific charge, Δq_m , and the initial specific charge, q_{m0} , as a function of the external electric field, E_{ex} . These experimental results were obtained using the manganese ferrite particles and the stainless steel plate with a 65-mm upper electrode. This figure indicates that the transferred specific charge has a linear relationship with the initial specific charge irrespective of the external electric field strength. The slopes were approximately -1 . As mentioned in Section 2.2, the transferred specific charge may be represented by Eq. (11), which shows that the transferred specific charge has a linear relationship with the initial specific charge. According to Eq. (12), the slope, a , is represented by the equation with an exponential function of the particle travel distance, L . Therefore, when L is sufficiently large, the slope, a , approximates to -1 . Because all of the slopes in Fig. 8 were approximately -1 , the charges on particles were considered to be almost in equilibrium. Furthermore, according to Eq. (11), we found that $q_{m\infty} = q_{m0}$ at $\Delta q_m = 0$, i.e., the equilibrium specific charge, $q_{m\infty}$, can be obtained from

the x -intercept.

Fig. 9 shows the relationship between the transferred specific charge, Δq_m , and the initial specific charge, q_{m0} , as a function of the particle travel distance, L . These results were obtained using the glass beads and the stainless steel plate under the condition of 0.1 MV/m. This figure indicates that the absolute value of the slope increases with increasing particle travel length. The characteristic length, L_0 , can be calculated from the slope, a , and the particle travel length, L , as shown in Eq. (14). Here, the slope, a , was determined from the experimental values of the transferred specific charge corresponding to the initial specific charge. Therefore, the characteristic length, L_0 , can be obtained without changing the travel distance of particles. For example, when the particle travel length, L , is 40 mm, and the slope, a , is -0.55 , as shown in Fig. 9, the characteristic length, L_0 , evaluates to 50 mm. Furthermore, based on the x -intercepts, the equilibrium specific charge, $q_{m\infty}$, is determined to be $-36 \mu\text{C}/\text{kg}$. This is a unique method that is used to quantitatively evaluate the particle tribocharging.

4.4. Equilibrium specific charge and external electric field

Fig. 10 shows the relationship between the equilibrium specific charge, $q_{m\infty}$, and the external electric field, E_{ex} . These experimental results were obtained using a combination of two types of particles and walls. We found that the equilibrium specific charge has a linear relationship with the external electric field, although the values depend on the materials. These experimental results can be explained by Eq. (10). When the equilibrium specific charge, $q_{m\infty}$, is zero, the following equation is derived, i.e.,

$$E_{\text{ex}0} = -\frac{V_c}{k_{\text{ex}} z_0} \quad (17)$$

where $E_{\text{ex}0}$ is the characteristic electric field, which is related to the inherent properties of the contact surfaces because the surface charges do not affect them. The determined values of $E_{\text{ex}0}$ are summarized in **Table 2**.

4.5. Characteristic value indicating the rate of particle tribocharging

We can determine the characteristic number, n_0 , as well as the characteristic value, L_0 , using the following equation.

$$n_0 = \frac{L_0}{d}, \quad (18)$$

where d is the average bounce distance, whose value can be determined by observation through the high-speed microscope camera. These characteristic values, L_0 , n_0 , and d , are summarized in Table 2.

The rate of particle tribocharging caused by repeated contact may be affected by the resistivity of materials; however, the details were not fully understood. The resistivity values of the stainless steel and the 25- μm -thick polyimide film used in this experiment were $\sim 10^{-6}$ (nominal value) and $1.5 \times 10^6 \Omega \text{ m}$ (measured value), respectively. The resistivity values of the particles used ranged from 65 to $4.5 \times 10^6 \Omega \text{ m}$, as shown in Table 1. We found that the resistivity of the particles and the plate synergistically affect the rate of particle tribocharging. **Fig. 11** shows the relationship between the characteristic number, n_0 , and the product of the resistivities of the particles and the plate. A positive correlation is seen in this figure. For high-resistance materials, the charges on the particles are generally difficult to flow; thus, the surface charge density tends to be inhomogeneous. To charge the particles completely, the particles need to contact the plate many times. In contrast, for low-resistance materials, the particles can be efficiently and homogeneously charged owing to the flow of the surface charges. In particular, when conductive materials such as metal particles contact an electrode, the charges on the particles are completely homogeneous. This phenomenon, known as induction charging, is immediately completed; however, the particle charging in this experiment progressed gradually. Therefore, although the mechanism of induction charging cannot be directly applied to our experimental results, the correlation between the characteristic number and the resistivity implies the possibility of surface charge flow. Although

further analysis is needed for a full understanding, this will be a task for future research.

5. Conclusion

We developed a new method to effectively characterize particle tribocharging caused by repeated contact with the plate in an external electric field. The system used for this characterization consists of the two inclined vibrating plates and electrodes, which enables us to control the mass flow rate and the initial charge of particles before measuring the charge transferred from the plate to the particles. Theoretically analyzing the initial and transferred charges and taking into account the movement of particles on the vibrating plate, we obtained the following results:

- 1) The values of the transferred specific charge obtained by the time integration of the electric current that was measured online at the second inclined vibrating plate agreed reasonably well with the difference between the specific charges of particles at the lower and upper ends of the vibrating plate; i.e., we verified that the charge balance in this system holds. Therefore, the simultaneous measurement of the electric currents generated at the vibrating plate and the charge on particles after passing through the vibrating plate enables us to simplify the experimental procedure.
- 2) The particle tribocharging can be evaluated based on the results of the particle charge profile, i.e., the relationship between the specific charge and the length of the electrode as a function of the external electric field and initial specific charge. The particle charge profile may be expressed as an exponential function, and can be characterized by the equilibrium specific charge and the characteristic length (or characteristic number), which indicates the rate of particle tribocharging caused by repeated contact.
- 3) The equilibrium specific charge can be obtained from the initial specific charge under the condition that the transferred specific charge is zero.

- 4) The equilibrium specific charge and the characteristic length can be calculated analytically from the relationship between the transferred specific charge and the initial specific charge without changing the travel distance of particles.
- 5) The characteristic number, which depends on the resistivity of the particles and the plate, is obtained from the characteristic length and average bounce distance.

Acknowledgement

This research was supported in part by a Grant-in-Aid for Scientific Research (B) (No. 26289288) from the Japan Society for the Promotion of Science (JSPS).

Nomenclature

a	slope of linear function	(–)
b	y-intercept of a linear equation	(C/kg)
C	capacitance between contact surfaces	(F)
D_p	particle diameter	(m)
D_{p50}	count median diameter of particles	(m)
d	average bounce distance	(m)
E_{ex}	electric field	(V/m)
E_{ex0}	electric field for $q_{mv0} = 0$	(V/m)
I	electric current	(A)
k_b	constant in Eq. (3)	(1/F)
k_c	constant in Eq. (5), i.e., charging efficiency	(–)
k_e	constant in Eq. (2)	(1/F)
k_{ex}	constant in Eq. (4)	(–)
L	length of electrode or travel distance of particles	(m)
L_0	characteristic length of particle tribocharging	(m)

M_t	total mass of particles	(kg)
m_p	mass of a particle	(kg)
n	number of particle-wall contacts	(-)
n_0	characteristic number of particle tribocharging	(-)
q	charge on a particle	(C)
q_m	specific charge, i.e., charge-to-mass ratio	(C/kg)
Δq_m	transferred specific charge	(C/kg)
q_{m0}	initial specific charge	(C/kg)
$q_{m\infty}$	equilibrium specific charge	(C/kg)
q_0	initial charge of a particle	(C)
q_∞	equilibrium charge of a particle	(C)
t	time	(s)
V	total potential difference	(V)
V_b	potential difference arising from space charge	(V)
V_c	contact potential difference based on surface work functions	(V)
V_e	potential difference arising from image charge	(V)
V_{ex}	potential difference arising from external electric field	(V)
w_p	mass flow rate of particles	(kg/s)
y	displacement of vibration	(m)
z_0	critical gap between contact surfaces	(m)

Greek letters

ϵ_0	absolute permittivity of gas	(F/m)
ρ_e	volume resistivity	(Ω m)
ρ_p	particle density	(kg/m ³)
σ_g	geometric standard deviation of particle diameter	(-)

References

- [1] S. Matsusaka, H. Masuda, Electrostatics of particles, *Adv. Powder Technol.* 14 (2003) 143–166.
- [2] S. Matsusaka, H. Maruyama, T. Matsuyama, M. Ghadiri, Triboelectric charging of powders: a review, *Chem. Eng. Sci.* 65 (2010) 5781–5807.
- [3] I. Adhiwidjaja, S. Matsusaka, S. Yabe, H. Masuda, Simultaneous phenomenon of particle deposition and reentrainment in charged aerosol flow — effects of particle charge and external electric field on the deposition layer, *Adv. Powder Technol.* 11 (1999) 221–233.
- [4] J. Yao, Y. Zhang, C-H. Wang, S. Matsusaka, H. Masuda, Electrostatics of the granular flow in a pneumatic conveying system, *Ind. Eng. Chem. Res.* 43 (2004) 7181–7199.
- [5] F.Y. Leong, K. A. Smith, C.-H. Wang, S. Matsusaka, J. Hua, Electrostatic effects on inertial particle transport in bifurcated tubes. *AIChE J.* 55 (2009) 1390–1401.
- [6] A. Sowinski, A. Mayne, P. Mehrani, Effect of fluidizing particle size on electrostatic charge generation and reactor wall fouling in gas–solid fluidized beds, *Chem. Eng. Sci.* 71 (2012) 552–563.
- [7] E.W.C. Lim, Mixing behaviors of granular materials in gas fluidized beds with electrostatic effects, *Ind. Eng. Chem. Res.* 52 (2013) 15863–15873.
- [8] E. Šupuk, A. Hassanpour, H. Ahmadian, M. Ghadiri, T. Matsuyama, Tribo-electrification and associated segregation of pharmaceutical bulk powders, *KONA Powder and Particle J.* 29 (2011) 208–223.
- [9] T.B. Jones, J.L. King, *Powder Handling and Electrostatics: Understanding and Preventing Hazards*, Lewis, Chelsea, 1991.
- [10] L. B. Schein, *Electrophotography and Development Physics*, 2nd ed. Springer-Verlag, Berlin/Laplacian Press, 1992/1996.
- [11] W. Kleber, B. Makin, *Triboelectric powder coating: a practical approach for industrial use*,

- Particul. Sci. Technol. 16 (1998) 43–53.
- [12] G.Q. Wu, J. Li, Z.M. Xu, Triboelectrostatic separation for granular plastic waste recycling: a review, *Waste Manage.* 33 (2013) 585–597.
- [13] R.K. Dwari, S.K. Mohanta, B. Rout, R.K. Soni, P.S.R. Reddy, B.K. Mishra, Studies on the effect of electrode plate position and feed temperature on the tribo-electrostatic separation of high ash Indian coking coal, *Adv. Powder Technol.* (in press) <http://dx.doi.org/10.1016/j.appt.2014.08.001>.
- [14] B.A. Grzybowski, A. Winkleman, J.A. Wiles, Y. Brume, G.M. Whitesides, Electrostatic self-assembly of macroscopic crystals using contact electrification, *Nat. Mater.* 2 (2003) 241–245.
- [15] S. Matsusaka, H. Masuda, Simultaneous measurement of mass flow rate and charge-to-mass ratio of particles in gas–solids pipe flow, *Chem. Eng. Sci.* 61 (2006) 2254–2261.
- [16] S. Matsusaka, H. Fukuda, Y. Sakura, H. Masuda, M. Ghadiri, Analysis of pulsating electric signals generated in gas-solids pipe flow, *Chem. Eng. Sci.* 63 (2008) 1353–1360.
- [17] C. He, X.T. Bi, J.R. Grace, Contact electrification of a novel dual-material probe with charged particulate flow, *Powder Technol.* 253 (2014) 1–9
- [18] T. Oguchi, M. Tamatani, Contact electrification phenomena and powder surface treatments, *Wear* 168 (1993) 91–98.
- [19] P.M. Ireland, Triboelectrification of particulate flows on surfaces: Part I–Experiments, *Powder Technol.* 198 (2010) 189–198.
- [20] J. Yao, J. Wu, Y. Zhao, E. W. C. Lim, P. Cao, F. Zhou, C.-H. Wang, N. Li, Experimental investigations of granular shape effects on the generation of electrostatic charge, *Particuology* 15 (2014) 82–89.
- [21] H.C. Hamaker, The London-van der Waals attraction between spherical particles, *Physica* 4 (1937) 1058–1072.
- [22] T. Matsuyama, H. Yamamoto, The electrostatic force between a charged dielectric particle and a conducting plane, *KONA Powder and Particle J.* 16 (1998) 223–227.

- [23] T. Matsuyama, H. Yamamoto, The electrostatic force between a partially charged dielectric particle and a conducting plane, *Part. Part. Syst. Charact.* 24 (2007) 1–6.
- [24] B. Techaumnat and T. Takuma, Analysis of the electrostatic force on a dielectric particle with partial charge distribution, *J. Electrostat.* 67 (2009) 686–690.
- [25] S. Matsusaka, D. Wei, M. Yasuda, S. Sasabe, Adhesive strength distribution of charged particles on metal substrate in external electric field, *Adv. Powder Technol.* (in press).
- [26] S. Matsusaka, K. Yamamoto, H. Masuda, Micro-feeding of a fine powder using a vibrating capillary tube, *Adv. Powder Technol.* 7 (1996) 141–151.
- [27] W. Theerachaisupakij, S. Matsusaka, M. Kataoka, H. Masuda, Effects of wall vibration on particle deposition and reentrainment in aerosol flow, *Adv. Powder Technol.* 13 (2002) 287–300.
- [28] Y. Higashiyama, Y. Ujiie, K. Asano, Triboelectrification of plastic particles on a vibrating feeder laminated with a plastic film, *J. Electrostat.* 42 (1997) 63–68.
- [29] E. Šupuk, C. Seiler, M. Ghadiri, Analysis of a simple test device for tribo-electric charging of bulk powders, *Part. Part. Syst. Charact.* 26 (2009) 7–16.
- [30] T. Akashi, M. Imba, T. Matsuyama, J. Ida, H. Yamamoto, Evaluation of electrostatic charging of particles in a metal shaker, *J. Soc. Powder Technol. Jpn.* 30 (2013) 845–850.
- [31] S. Matsusaka, M. Oki, H. Masuda, Control of electrostatic charge on particles by impact charging, *Adv. Powder Technol.* 18 (2007) 229–244.
- [32] S. Matsusaka, K. Ando, Y. Tanaka, Development of electrostatic charge controller for particles in gases using centrifugal contact, *J. Soc. Powder Technol. Jpn.* 45 (2008) 380–386.
- [33] S. Matsusaka, Control of particle tribocharging, *KONA Powder and Particle J.* 29 (2011) 27–38.
- [34] P. Bunchatheeravate, J. Curtis, Y. Fujii, S. Matsusaka, Prediction of particle charging in a dilute pneumatic conveying system, *AIChE J.* 59 (2013) 2308–2316.
- [35] S. Matsusaka, T. Nishida, Y. Gotoh, H. Masuda, Electrification of fine particles by impact on

- a polymer film target, *Adv. Powder Technol.* 14 (2003) 127–138.
- [36] Matsusaka, S., J. Iyota, M. Mizutani and M. Yasuda, Characterization and control of particles triboelectrically charged by vibration and external electric field, *J. Soc. Powder Technol. Jpn.* 50 (2013) 632–639.
- [37] M. Mizutani, K. Takeda, M. Yasuda, S. Matsusaka, Characterization of particles triboelectrically charged by a two-stage system using vibration and external electric field, *J. Soc. Powder Technol. Jpn.* 50 (2013) 832–839.
- [38] S. Matsusaka, M. Kobayakawa, Y. Hosoh, M. Yasuda, Micro-feeding of fine powders using vibration shear flow, *J. Soc. Powder Technol. Jpn.* 49 (2012) 658–662.
- [39] S. Matsusaka, M. Kobayakawa, T. Yamamoto, M. Yasuda, Analysis of vibration shear flow of fine powders, *J. Soc. Powder Technol. Jpn.* 49 (2012) 663–668.

Table 1 Size distributions and physical properties of the particles

	Glass	Manganese ferrite	Manganese ferrite coated with polymer
$D_{p50}^{(0)}$ (μm)	101	81	82
σ_g (μm)	1.1	1.2	1.2
ρ_p (kg/m^2)	2.5×10^3	4.8×10^3	4.7×10^3
ρ_e ($\Omega \text{ m}$)	4.5×10^6	65	2.6×10^5

Table 2 Characteristic values determined experimentally

Plate	Particle	$E_{\text{ex}0}$ (MV/m)	L_0 (mm)	n_0	d (mm)
Stainless steel	Manganese ferrite	0.02	18	11	1.6
	Manganese ferrite coated with Polymer	0.23	41	22	1.9
	Glass	0.03	50	38	1.3
Polyimide	Manganese ferrite	-0.1	190	100	1.9
	Manganese ferrite coated with Polymer	0.22	620	260	2.4

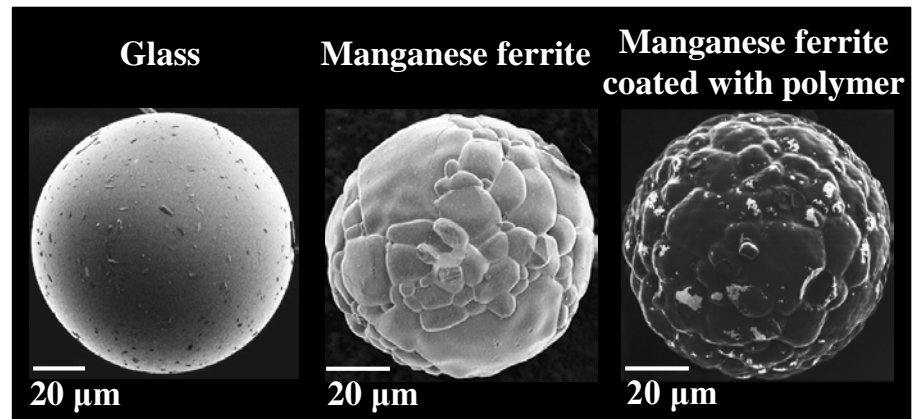


Fig. 1. SEM images of particles.

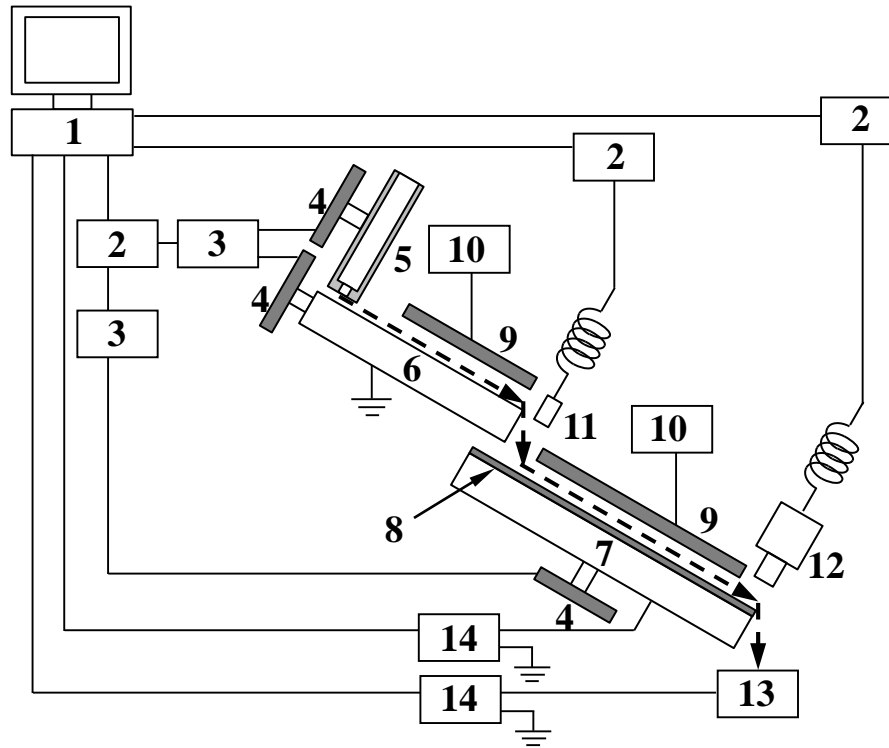


Fig. 2. Schematic diagram of the setup (1. computer; 2. controller; 3. amplifier; 4. piezoelectric vibrator; 5. short pipe filled with particles; 6. first vibrating plate (lower electrode); 7. second vibrating plate (lower electrode) 8. removable material; 9. upper electrode; 10. power supply; 11. laser vibrometer; 12. high-speed camera; 13. faraday cup; 14. electrometer).

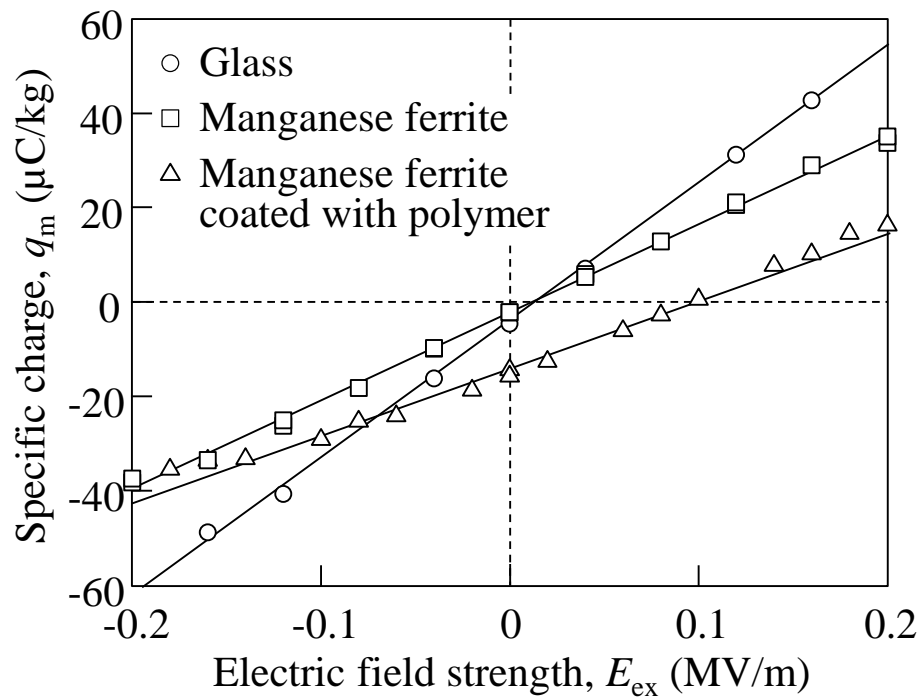


Fig. 3. Variation of specific charge of particles at the first plate (stainless steel plate).

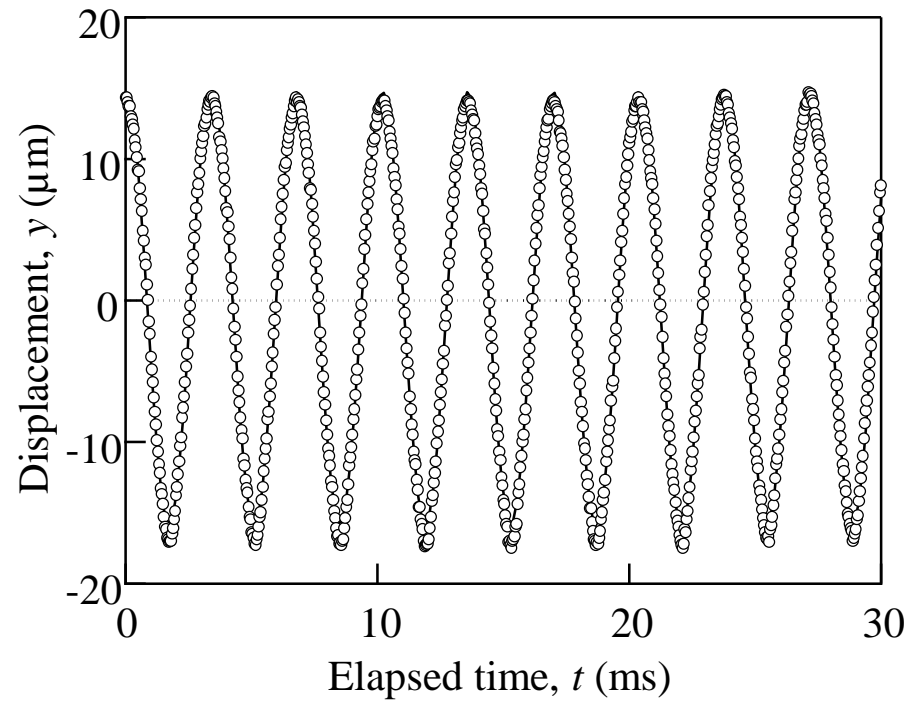


Fig. 4. Displacement of the second inclined vibrating plate as a function of time.

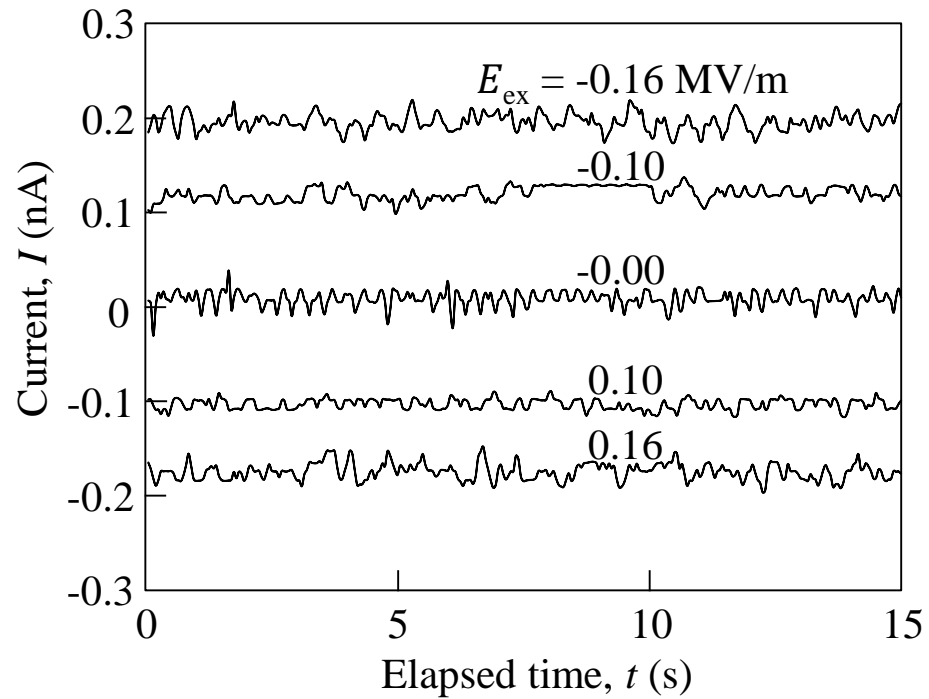


Fig.5. Electric currents detected from the second vibrating plate (Manganese ferrite particles, stainless steel plate, $L = 65$ mm).

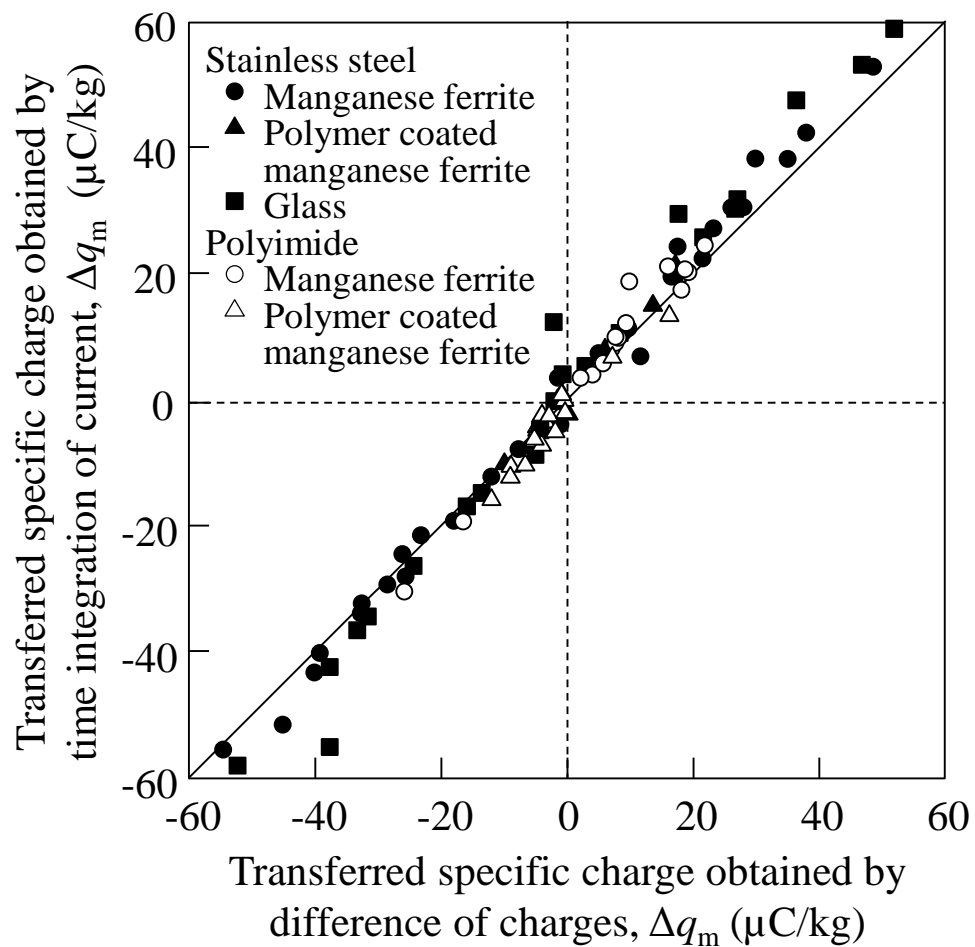


Fig. 6. Comparison of the transferred specific charges obtained by the time integration of the electric current and the difference in the charges measured by a Faraday cup.

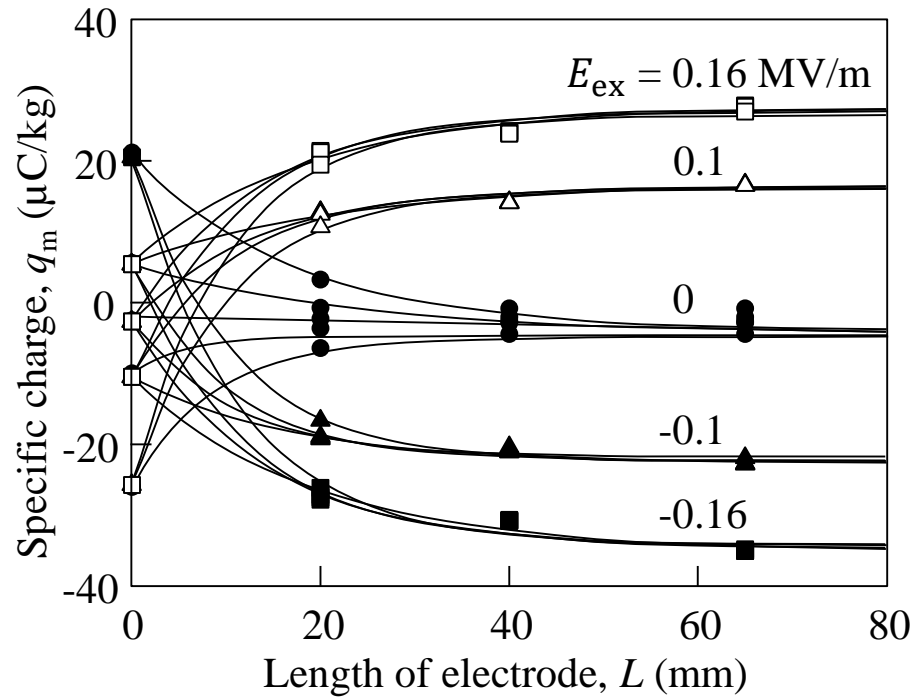


Fig.7. Particle charge profiles (Manganese ferrite particles, stainless steel plate).

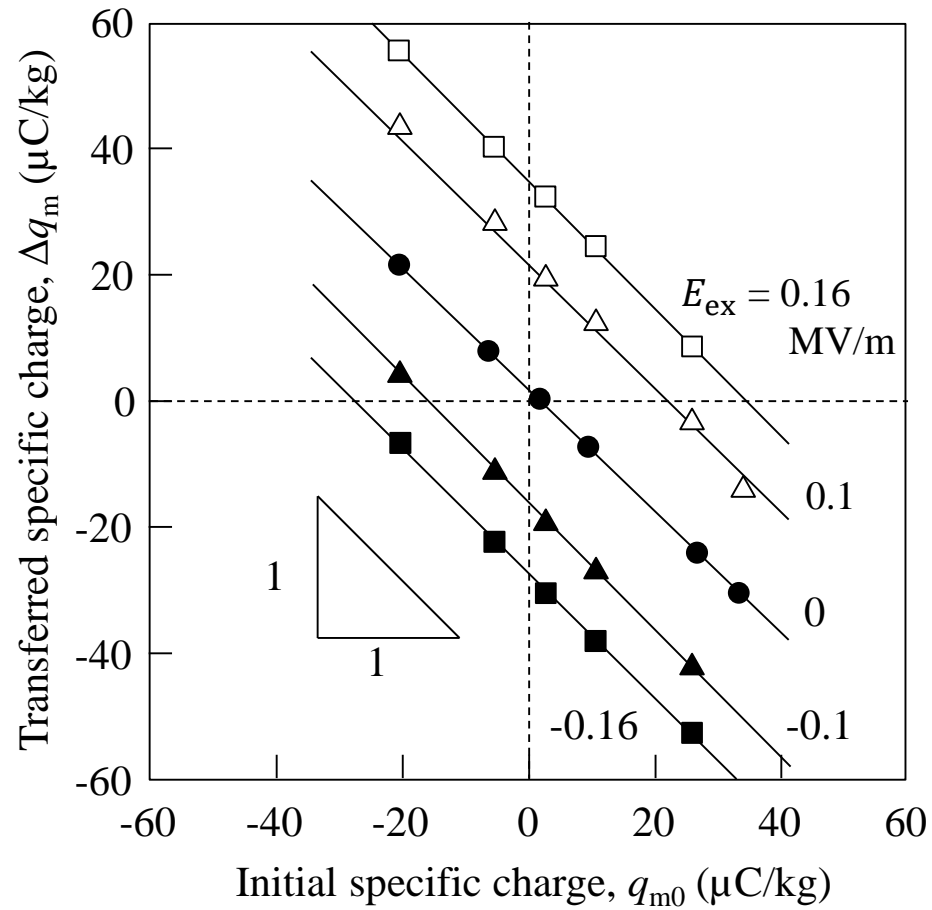


Fig.8. Relationship between transferred specific charge and initial specific charge as a function of external electric field (Manganese ferrite particles, stainless steel plate, $L = 65$ mm).

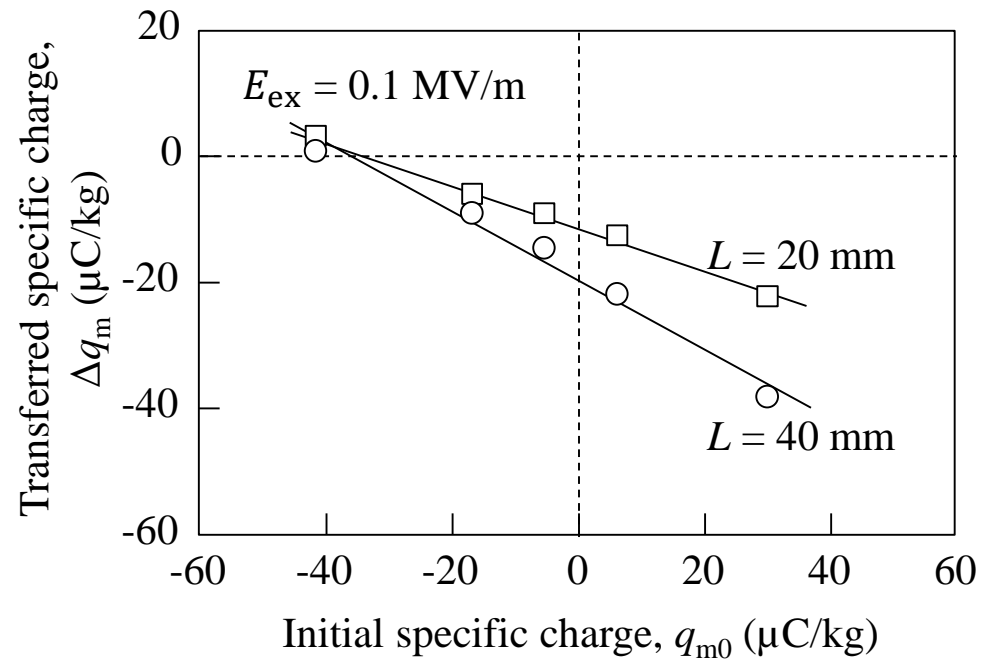


Fig. 9. Relationship between transferred specific charge and initial specific charge as a function of travel distance of particles (Glass beads, stainless steel plate).

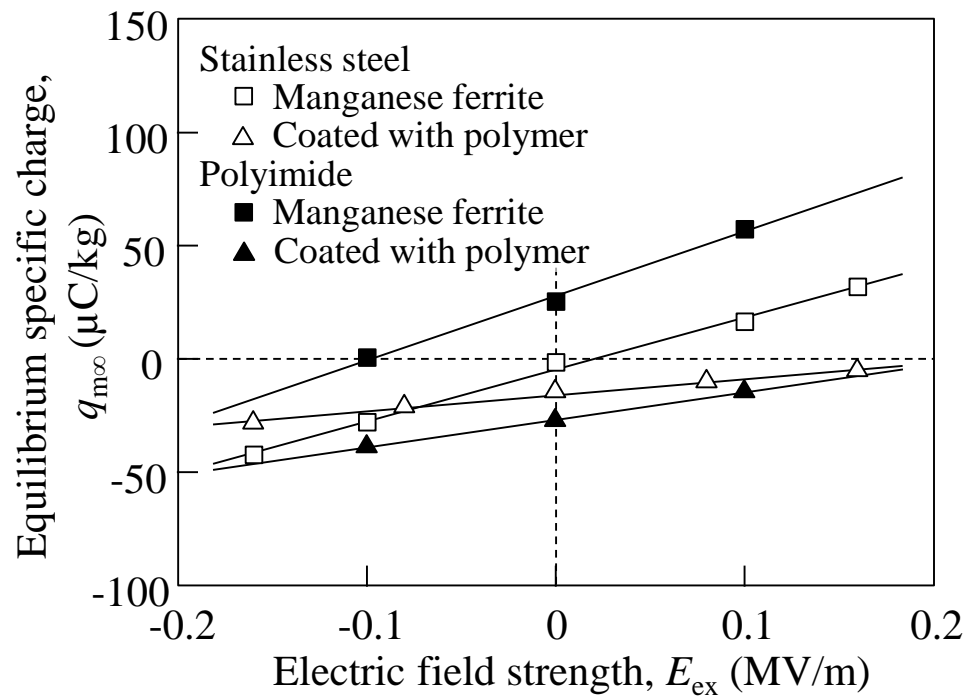


Fig.10. Relationship between equilibrium specific charge and external electric field.

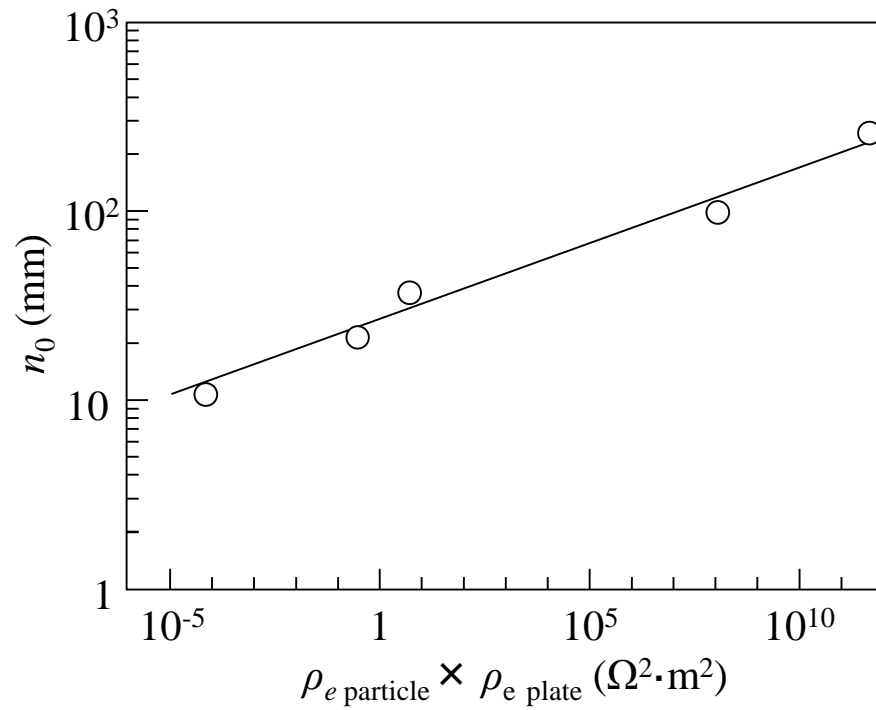


Fig.11. Characteristic number of particle electrification.